

# PERFORMANCE TESTS OF THE PHOTON MONOCHROMATOR FOR SELF-SEEDED AT FLASH \*

R. Treusch, U. Hahn, J. Viefhaus, DESY, Hamburg, Germany

H.K. Bechtold, J. Hartvig, H. Juul, V. Toft, Aarhus University, Aarhus, Denmark

S.V. Hoffmann ISA, Aarhus, Denmark

C. Knöchel, LBNL, Berkeley, California, U.S.A.

R. Reininger, Scientific Answers & Solutions, Madison, Wisconsin, U.S.A.

R. Follath, G. Reichardt, F. Senf, F. Siewert, BESSY GmbH, Berlin, Germany

## Abstract

A single pass FEL amplifier can produce extremely intense and fully coherent radiation at short wavelengths if it is seeded by a coherent light beam resonant with the magnetic structure and collinear with the electron beam. Since at the present time a single pass SASE<sup>1</sup> FEL is the only source of sufficiently intense, tunable radiation in the soft X-ray region, it has been proposed to use such a source in combination with a narrow-band monochromator for seeding an FEL amplifier [1]. By means of such a "Self-Seeding", the soft X-ray free electron laser FLASH [2] at DESY will be modified so that it can provide coherent radiation in space *and* time in a wavelength range from about 60–6 nm ( $\approx 20\text{--}200$  eV).

Here, we will focus on the performance of the photon monochromator beamline for the seeding which was set up and tested at the synchrotron radiation storage ring ASTRID in Aarhus. The optical and mechanical design will be described along with results on the resolving power of the monochromator which have been obtained scanning across rare gas resonance lines at various energies.

## INTRODUCTION

Since August 2005 FLASH is providing SASE radiation for users, presently tunable from about 47–13 nm and soon from 60 down to 6 nm. The pulses possess a pulse length of a few 10 fs, almost full transverse coherence, limited longitudinal (temporal) coherence and pulse energies from about 10–100  $\mu\text{J}$ . By means of the Self-Seeding (or *Seeding Option*) FLASH will be modified in a way that it can provide fully longitudinally coherent, narrow-bandwidth radiation. The output radiation will then exhibit all the characteristic properties of conventional optical lasers but at much shorter wavelengths and with a continuous tunability between 6 and 60 nm. The enhanced beam properties will extend the range of possible applications, particularly for high resolution spectroscopy and for all experiments which need full longitudinal coherence.

The Self-Seeding consists of an additional undulator section, a bypass for electrons and a photon monochromator beamline. R&D in undulator design, FEL theory and elec-

tron beam dynamics, as well as on photon beam propagation and optical components were important parts of the project. The photon monochromator beamline aspect will be detailed here. More details, also on all the other components can be found in [3].

The general layout of the Self-Seeding is sketched in figure 1. The first undulator operates in the SASE mode

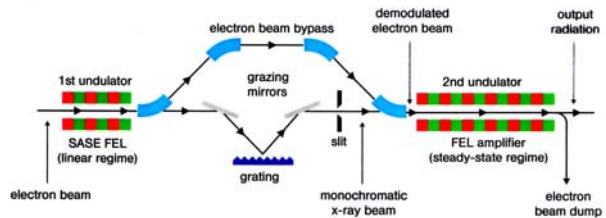


Figure 1: Schematic setup (side view) of the Self-Seeding for FLASH. Behind the first undulator, FEL radiation and electrons are separated. While the electrons travel through the bypass represented by the four blue dipole magnets in the upper part of the figure, the photons propagate across the photon monochromator beamline below in order to provide a narrow-bandwidth seed that is overlayed with the electrons again at the entrance of the second undulator.

in the "linear" (= exponential gain) regime, about 2–3 orders of magnitude below saturation. It produces intense, but structured light pulses as shown in the left part of figure 2. Subsequently electrons and photons are separated. Before they are overlayed again in the second undulator, the electrons travel through a magnetic chicane that is used to remove the longitudinal density modulation ("micro-bunching") of the electron beam which was induced by the FEL process in the first undulator. For the photons, a high resolution grating monochromator together with some matching optics is used as a narrow-band filter to provide the coherent radiation seed which is amplified to saturation in the second undulator section. The resulting spectral distribution is given in the right part of figure 2.

The requirements for the final seeding radiation pulse are obvious: its photon wavelength has to be within the gain bandwidth of the FEL amplifier, the photon bandwidth has to be narrow enough to provide a coherence length as long as the electron bunch length, and the intensity of the

\* Work funded through HGF-Strategiefonds (01SF9935/1)

<sup>1</sup>Self-Amplified Spontaneous Emission

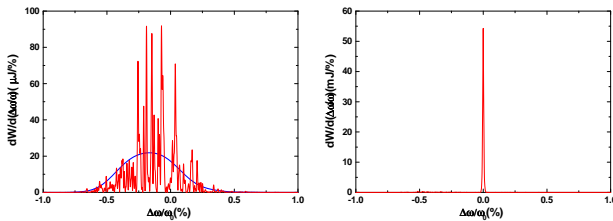


Figure 2: Simulated typical frequency spectrum of a single FEL pulse (from [1]). Left: behind the 1st undulator (SASE, 2 orders of magnitude below saturation). Right: at the exit of the 2nd undulator (seeded FEL in saturation).

seeding radiation has to be much larger than that of the shot noise<sup>2</sup> coming from density fluctuations in the electron beam. Successful seeding then yields a spectral brilliance of FLASH that is up to a factor of 100 higher, i.e. the output power of the seeded FEL is concentrated in a single line which is about a hundred times narrower than the spectrum of the conventional SASE FEL while the pulse energy at saturation remains approximately unchanged. In addition, the pulse now attains full longitudinal coherence.

## PHOTON MONOCHROMATOR BEAMLINE

The optical design of the photon beamline was performed applying computer programs that were partly developed for the Self-Seeding at FLASH [4, 5]. The programs combine standard ray tracing with a wavefront propagation of the simulated FEL beam from the end of the first undulator section across the optical elements of the beamline. The output wavefront was used as input for FEL simulations calculating the amplification process in the second undulator. This finally yielded numbers for the efficiency of the seeding process, i.e. the quality of the coupling of the seed pulse with the electron bunch.

In the final, optimized layout, the beamline consists of the monochromator, containing a premirror and a varied line spacing (VLS) spherical grating, and a pair of focusing mirrors at each side of the monochromator. To minimize the number of elements in the beamline, all the reflections and the diffraction are in the same plane. Beside the desired monochromator resolving power of  $E/\Delta E \approx 10000 - 20000$ , the optical system was designed such that it produces a 1:1 image of the (complex conjugated) wavefront at the entrance of the second undulator section. This way, the optimum coupling, i.e. best longitudinal and transverse overlap between the seed pulse and the electron bunch is achieved [1, 6]. The beamline optics were optimized for the short wavelength end at 6.4 nm and will work satisfactorily up to about 60 nm [7]. The calculated efficiency of the beamline in the wavelength range from 5.8 to 77 nm is better than 10% with carbon coated optics [8]. This en-

sures that the seed pulse delivered by the monochromator clearly dominates the shot noise in the second undulator and is amplified to saturation. Figure 3 depicts the layout of the beamline, while table 1 summarizes the parameters of the optical elements.

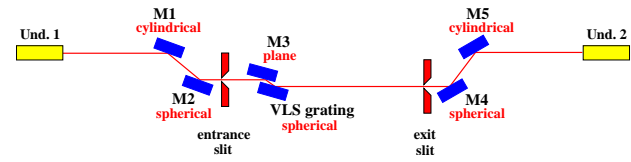


Figure 3: Layout of the photon monochromator beamline of the Seeding Option (side view). M1 to M5 denotes the mirrors. For better visibility, the mirror angles and vertical displacements are greatly exaggerated. The distance between undulator 1 and undulator 2 is 22 m, whereas the maximum vertical distance to the straight line (for the grating and M4) is about 135 mm only (cf. table 1).

Table 1: Parameters of the photon monochromator beamline for the Self-Seeding [7]. Horizontal position means left to right in fig. 3. Incidence angles are given with respect to the surface normal. Positions/angles for M3 and Grating are listed for both ends of the design scan range.

Component	Position (Hor./Vert.) [mm,mm]	Radius [mm]	Angle [Degree]
M1: cylindrical	4500 / 0	345.50 (sagittal)	87.50
M2: spherical	5844.86 / -117.66	$41.360 \times 10^3$	87.50
Entrance Slit	6844.86 / -117.66		
M3: plane	8879.75 / -117.66		86.56
	8946.89 / -117.66		83.52
Grating: VLS, spherical	9020.75 / -134.66	$6.0457 \times 10^6$	88.28
			86.77
Exit Slit	15552.1 / -134.66		
M4: spherical	16502.1 / -134.66	$25.70 \times 10^3$	86.16
M5: cylindrical	17500 / 0	530.75 (sagittal)	86.16
Start Und. 2:	22000 / 0		

### Layout of the mirror chambers

Due to the tight space, the mirror chamber design had to be very compact. It was decided to have all movements of the mirrors outside the vacuum chamber, in order to avoid a production of particles in the vacuum arising from friction of moving parts inside the chamber. From the stringent requirements of positioning accuracy in the  $\mu\text{m}$  and sub-mrad range it followed that one needs a very good resolution of the individual movements, in particular the adjustment of beam incidence angle (pitch), and a good reproducibility of the position settings. All, at most six, degrees of freedom had to be “orthogonal”, i.e. decoupled. This demanded high precision bearings, translation slides etc., a precise mounting and a robust construction. In the final design, all movements were realized with a twofold suspension, as symmetric to the center of the mirror as possible. Figure 4 shows an exploded view of the mirror chamber for mirror M1. The four mirror chambers for M1, M2, M4 and M5 are, apart from minor differences regarding the mirror holder, almost identical and based on a tested prototype.

<sup>2</sup>= spontaneous undulator emission along the first few gain lengths

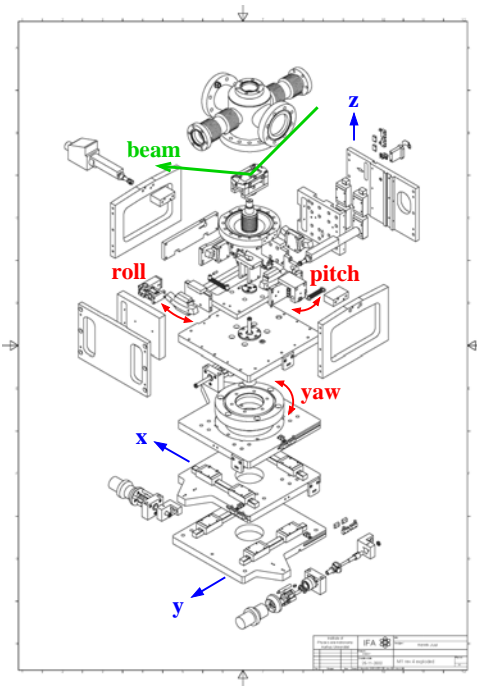


Figure 4: Exploded view of the setup for mirror manipulation used for M1, M2, M4 and M5, including the vacuum chamber. In the lower half one sees stacked tables for x-, y- and yaw-movements which move the complete vacuum chamber, including the mirror. The upper half shows nested roll, pitch and z-movements that manipulate the mirror inside the vacuum chamber through a feedthrough connected with bellows.

### Layout of the monochromator

The monochromator is the most crucial component of the beamline with respect to alignment accuracy and desired resolution of the movements [3]. In particular, the required precision and resolution of the pitch of the pre-mirror M3 and the grating made it necessary to put these two rotations inside the vacuum chamber and to attach *state of the art* angle encoders with sub- $\mu$ rad resolution<sup>3</sup> right at the corresponding axes, similar to some commercially available designs. The basic principle for the movements of the monochromator was adopted from a patented layout [9] that has been applied for high resolution plane grating monochromators. Among its several advantages, this design has a wavelength independent magnification along the dispersion direction. The optical principles of the current monochromator are however, different. The focusing and higher order aberration corrections are achieved with only two elements, the plane mirror (M3) and the variable line spacing spherical grating (a more detailed discussion of the basic principles of the monochromator can be found in refs. [10, 11]). The mechanics for changing the monochromator wavelength setting consist of two nested but separately suspended “cradles” for the grating and M3

which are rotated via external movers that push/pull the respective lever arm of each cradle (Figure 5). High precision radial bearings<sup>4</sup> are employed for the suspension to guarantee the precision and rigidity of the rotational axes.

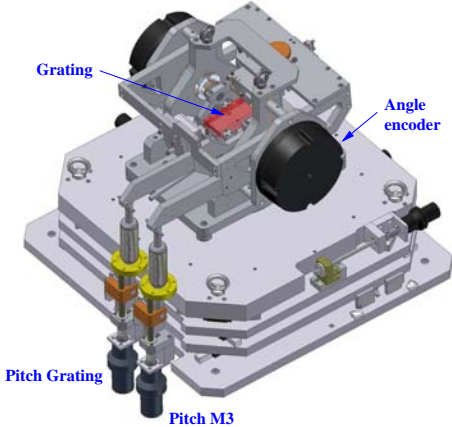


Figure 5: Drawing of the monochromator mechanics showing both, the in vacuum pitch movements via bellow-coupled linear feedthroughs as well as the external stacked tables for x-,y- and yaw-movements. The vacuum chamber mounted on the uppermost table has been omitted.

In order to span the wavelength range from 6-60 nm with proper imaging properties and resolving power including some overlap, one needs three gratings with 800 lines/mm ( $\approx 4.5$ –16 nm), 356 lines/mm (10–36.5 nm) and 160 lines/mm (from about 22 to even 83 nm). In contrast to the usual approach with three gratings on independent substrates, we decided to go with three holographically produced gratings side by side on a common spherical Si substrate. That way, the manufacturer (Zeiss) could already – and much better than with individually aligned gratings – ascertain that all gratings are nicely parallel to one another and have all the same incidence (pitch) angle as well as the same roll angle. The perfect optical quality of the gratings regarding parameters such as slope errors, radius of curvature and groove density variation – without and also within the grating holder – was verified at BESSY with the latest generation of nanometrology devices [12].

## MONOCHROMATOR PERFORMANCE

In order to test the monochromator performance, in particular its resolving power, the beamline was set up at ASTRID from M1 down to the exit slit (without M4 and M5). A photoionization chamber (gas cell) was put just behind the exit slit to measure the energy dependent ionization of rare gases by monitoring the ion current. Scanning across resonances with linewidths of 1 meV and below – as in the case of doubly excited Helium around 64 eV – directly reveals the resolving power of the monochromator [13]. Other rare gas resonances, e.g. from

<sup>3</sup>Heidenhain RON905 UHV

<sup>4</sup>custom-made by Mahr, Göttingen, Germany

Argon (around 244–250 eV) and Krypton (91–95 eV) with widths of few ten to more than one hundred meV only allow to estimate a lower limit of the resolving power at these energies while still being very useful for accurate energy calibration.

Figure 6 shows a scan across the He resonances after proper alignment and optimization of the beamline at ASTRID. The width of the narrow resonances (e.g.  $n=7+, 8+$ ) of only  $(3.5 \pm 0.5)$  meV yields a resolving power of  $E/\Delta E \simeq 19,000$  and is in very good agreement with the respective simulations [14]. Some more results are summarized in figure 7 in comparison to the simulations. Even without a final optimization of all the beamline settings – which would have required a more detailed survey of all degrees of freedom – we reached 90 % of the expected values and surpassed the requirements for the seeding at these energies by about a factor of two already. In addition, the

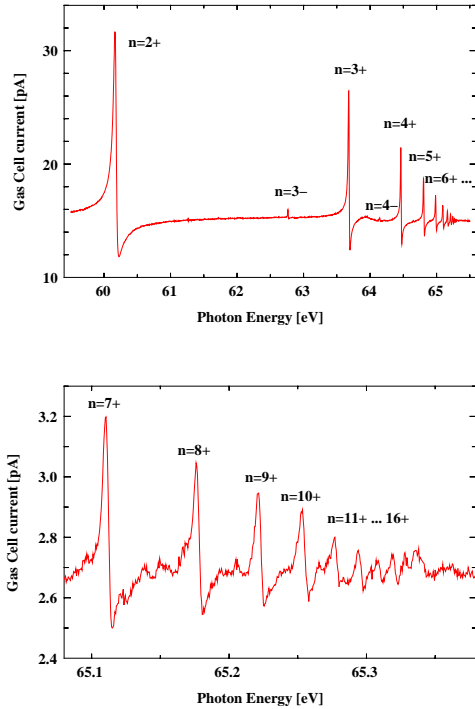


Figure 6: Photoionization yield scan across the He  $1P_0$  resonances (raw data without further normalization). The lower figure is a zoom into the tail of the Rydberg-series ( $n=7+$  to continuum) of the upper figure.

aforementioned common grating substrate very much simplified alignment and operation, as expected. When, e.g., changing after proper energy calibration from one grating to another, the relative energy setting on the new grating was typically 0.2–0.5 % (some 10 meV) off.

Based on our results we conclude that the monochromator beamline is mechanically very stable, precise, reproducible and fully within its specifications with resolving powers between 10000 and 20000, i.e. bandwidths of a few meV only. It meets all requirements for the Self-Seeding.

We would like to acknowledge the technical support FEL Technology II

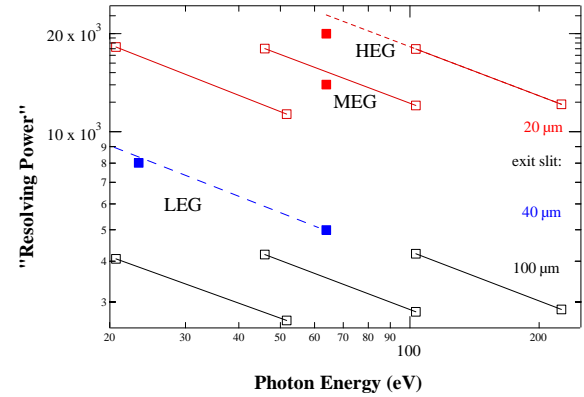


Figure 7: Summary of the measured resolving power. Filled squares: data from resonance measurements, empty squares: simulation results [14] incl. lines to guide the eye. HEG/MEG/LEG=high/medium/low energy grating (800/356/160 lines/mm), respectively.

from the HASYLAB(DESY) experiment controls and vacuum groups and all the colleagues in the ISA workshops that manufactured most of the beamline mechanics and the vacuum chambers.

## REFERENCES

- [1] J. Feldhaus et al., Opt. Commun. **140**, 341-352 (1997)
- [2] W. Ackermann et al., Nature Photonics **1**, 336-342 (2007)
- [3] R. Treusch, *The Seeding Option for the VUV Free Electron Laser at DESY, Final Report*, DESY, Hamburg (2003), available on request (rolf.treusch@desy.de)
- [4] R. Reininger et al., AIP Conf. Proc. **521**, 458-462 (1999)
- [5] R. Reininger et al., Nucl. Instr. and Meth. A **467-468**, 38-41 (2001)
- [6] E.L. Saldin et al., Nucl. Instr. and Meth. A **445**, 178-182 (2000)
- [7] R. Reininger, *Optics parameters of the beamline for the seeded FEL*, Internal Project Report (2001), Ref. B7 on the CD-ROM of Ref.[3]
- [8] R. Reininger, *VLS grating efficiencies and gratings specifications for the seeded FEL beamline*, Internal Project Report (2002), Ref. B9 on CD-ROM of Ref.[3]
- [9] German patent No. 3045931, U.S. patent 4,490,041, see als: H. Petersen et al., Rev. Sci. Instrum. **66**(1), 1-14 (1995)
- [10] R. Reininger, *A study of possible PGM beamlines for the seeded SASE free electron laser*, Internal Project Report (1999), Ref. B2 on CD-ROM of Ref.[3]
- [11] R. Reininger, *A varied line-spacing spherical grating monochromator for the seeded SASE FEL*, Internal Project Report (1999), Ref. B3 on CD-ROM of Ref.[3]
- [12] F. Siewert et al., AIP Conf. Proc. **879**, Part 1, 667-670 (2006)
- [13] M. Domke et al., Physical Review A **53**, 1424-1438 (1996) and refs. therein
- [14] R. Reininger, *Expected performance of the seeding beamline at ASTRID*, Internal Project Report (2003), available on request (R.T.)